

Quantum Impurity Physics in Coupled Quantum Dots

Rok Žitko

Jožef Stefan Institute, Ljubljana, Slovenia

Janez Bonča

Faculty of Mathematics and Physics, University of Ljubljana, Ljubljana, Slovenia

Jožef Stefan Institute, Ljubljana, Slovenia

29th August 2007

Article outline

Glossary

1. Definition of the Subject and Its Importance
2. Introduction
3. Quantum dots as impurity systems
4. Theoretical tools
5. Quantum transport and Kondo physics
6. Competing physical effects
7. Universal behavior versus complex particularities
8. Future directions
9. Bibliography

Glossary

Quantum dot device: nanoscopic electronic device resembling a transistor which incorporates a quantum dot as the central active element; sometimes also called single electron transistor. A quantum dot is an extremely small puddle of electrons which can be considered as an artificial atom since the confinement of electrons leads to quantized energy levels: the electrons form orbitals much like the electrons in orbit around an atomic nucleus. Gate-defined semiconductor quantum dots provide precisely tunable physical realizations of quantum impurity models.

Quantum impurity system: system of a localized magnetic impurity in interaction with itinerant free electrons from a conduction band of an otherwise clean metal. It can be described using an idealized quantum impurity model such as Kondo or Anderson model.

Tunneling: transmission of electrons from one electrode to another through classically-forbidden potential barriers such as thin insulators or empty space. Tunneling is a characteristic quantum phenomenon that is commonly at play on the nanoscopic scale.

Kondo effect: Kondo effect is a many-particle effect which occurs in quantum impurity systems due to increased spin-flip scattering of the conduction band electrons on the magnetic impurity at low temperatures. It leads to various anomalies in thermodynamic and dynamic properties. In the context of the electronic transport through a quantum dot, the Kondo effect is reflected in enhanced conductance (zero-bias anomaly) at reduced temperatures.

Channel: In the context of impurity physics, a channel is a set of energy levels in the conduction band which are coupled to the impurity. Several independent channels may be coupled to a single impurity. In the context of quantum dots, the relevant channels may be identified with the conduction channels in the leads attached to the nanostructure, however the number of channels in the effective impurity problem may be lower than the number of physical conduction channels.

Quantum phase transition: A quantum phase transition is a zero-temperature phase transition triggered by tuning system parameters. While thermal phase transitions occur due to thermal fluctuations, quantum phase transitions emerge from zero-point quantum fluctuations in the ground state.

Particle-hole symmetry: Idealized impurity models exhibit particle-hole symmetry if the model remains unchanged when all occupied levels are mapped into unoccupied levels and vice versa. This occurs for half-filled systems, when precisely one electron occupies each impurity on the average.

1 Definition of the Subject and Its Importance

Advances in the field of nanoscience and nanotechnology empower us with new tools for probing electronic systems of increasingly small sizes. Nowadays one can, for example, measure electrical conduction of semiconductor quantum dots with lateral extent of a few 10 nm, single molecules, and even individual atoms trapped between two electrodes. Nanodevices of practical interest typically consist of an active element (such as a quantum dot [1, 2, 3]) weakly coupled to two conducting leads by tunneling junctions so that electric current can flow through the device. The active element confines a small number of electrons. Particularly interesting is the case where this number is an odd integer; the excess single electron is then unpaired and carries magnetic moment. It has been recently demonstrated that a quantum dot of this type behaves as an artificial magnetic atom which can be experimentally tuned using electrodes [4, 5, 6]. The advantage of performing experiments on such artificial atoms is that various effects that depend on the number of electrons can be studied simply by changing voltages applied on gate electrodes, rather than performing experiments on different chemical elements.

It is now possible to produce nanodevices consisting of a small number of quantum dots which are coupled by tunneling junction between each other and to external electrodes [7, 8, 9, 10, 11, 12]. Multiple quantum dot systems can be used to study various magnetic effects, such as antiferromagnetic and ferromagnetic ordering, Kondo screening, and other phenomena in which the role of electron-electron interactions is essential. This provides insight into the behavior of similar macroscopic magnetic systems and reveals how magnetic behavior scales from the atomic size. Furthermore, these devices are interesting in their own right as candidates for quantum information storage and processing. They represent the ultimate degree of miniaturization of electronic devices and they are likely to evolve into

the building blocks of the circuitry of tomorrow.

2 Introduction

Real metal is never an ideally clean and homogeneous material. Instead, any metal sample invariably contains a finite concentration of various impurities. Impurities affect resistivity of the metal particularly at low temperatures when electron scattering of thermal origin is suppressed and the residual scattering on static impurities determines at which value the resistivity ultimately saturates. It was remarked very early that in some samples the resistance after the initial decrease unexpectedly increases at the lowest temperatures: this behavior constitutes the “problem of the resistance minimum” [13]. Further experimental work indicated that such anomalies are due to the presence of magnetic impurities, such as iron, cobalt or manganese, in a non-magnetic metal host. Theoretical understanding was lacking until the work of J. Kondo in 1964 who had shown that the rate of scattering events in which the magnetic moment of the impurity is changed (magnetic or spin-flip scattering) surprisingly increases as the temperature is lowered [14]; this behavior of impurity systems became known as the Kondo effect. More detailed understanding became possible with the development of advanced theoretical tools based on the idea of the renormalization group by P. W. Anderson, K. G. Wilson and others [15].

Impurity models and the Kondo effect are widely studied for several reasons. The Kondo effect is one of the very few non-trivial many-particle effects where an intensive theoretical effort eventually resulted in a very good and detailed understanding. In fact, the Kondo problem was historically the primary motivation for the development of many widely applicable theoretical approaches and has driven the progress in the field of the many-particle physics for many decades. More generally, the impurity models have attracted the condensed matter community due to their unexpectedly complex and rich behavior. On a more practical level, Kondo physics plays an important role in many complex materials which may have practical applications. The Kondo screening of local moments namely competes with magnetic ordering; the result of this competition determines the magnetic properties of materials at low temperatures. Fermi and non-Fermi liquid behaviors, ferromagnetic and antiferromagnetic correlations, and diverse behavior of heavy fermion systems [16] are the outcome of the competition between the Kondo effect and magnetic exchange interaction [8].

More recently, the Kondo problem became popular due to the advances in the field of nanoscience and nanotechnology. It is now possible to perform electron transport measurements on very small systems, such as quantum dots [17], segments of carbon nanotubes [18], single molecules with an embedded magnetic ion [19] and in the extreme case even single magnetic atoms deposited on the surface of a normal metal [20, 21, 22]. The Kondo effect was predicted to occur in quantum dots in late 1980s [23, 24] and experimentally observed a decade later [4, 5]. Again, it was found that the Kondo effect leads to transport anomalies at low temperatures. By studying the Kondo physics in systems where parameters can be continuously tuned, we better understand systems where such control is not possible, as in the case of bulk materials. Quantum dot systems are thus a laboratory for studying various effects driven by strong electron correlations.

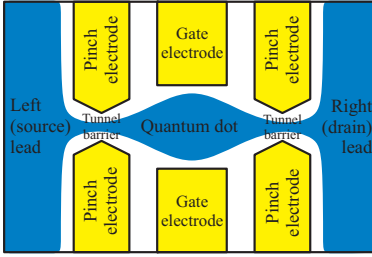


Figure 1: Schematic representation of a semiconductor quantum dot electrostatically defined by the voltages applied on surface metal gate electrodes.

3 Quantum dots as impurity systems

3.1 Semiconductor quantum dots

Particularly interesting devices are quantum dots patterned in high-quality semiconductor heterostructures. In heterostructures a subsurface layer of high-electron-mobility two-dimensional electron gas is confined near the interface between gallium arsenide (GaAs) and aluminum gallium arsenide (AlGaAs) [25]. Such crystal structures may be grown very accurately one atomic layer at a time by molecular beam epitaxy [26]. Lateral quantum dots [27] are then defined by patterning metallic gates on the sample surface (Fig. 1). Using a sufficiently negative gate voltage, the two-dimensional electron gas is depleted in the region below the electrode and a barrier is formed: quantum dot is said to be electrostatically defined. This “split-gate” technique is also used to build quantum point contacts, quantum wires and similar devices [28]. By changing the voltage on the pinch electrodes, the strength of the coupling of the dot with the electron gas in the leads is controlled. By applying voltage on the gate electrode near the quantum dot region, the number of electrons confined in the dot can be accurately tuned. Nowadays it is possible to fabricate few-electron quantum dots and exactly control the number of electrons starting from zero.

3.2 Quantum impurity models

An idealized quantum impurity model describes a single point-like impurity (a zero-dimensional defect) in an otherwise homogeneous host environment composed of a gas of particles that form a continuum of extended states. The impurity is assumed to have internal degrees of freedom (such as intrinsic angular momentum, or “spin”) and interacts with the continuum particles. A paradigmatic quantum impurity model is the Kondo model for a magnetic impurity atom, such as cobalt, embedded in a host metal which is non-magnetic, such as copper; the magnetic impurity interacts with the conduction band electrons via anti-ferromagnetic exchange interaction. Generalized quantum impurity models may involve several impurities or more complex, non-homogeneous environment. The theoretical significance of the quantum impurity models stems from their ubiquitous applicability to a vast array of physical systems such as bulk Kondo systems, heavy-fermion compounds and other strongly correlated systems, dissipative two-level systems, single magnetic impurities and quantum dots.

In nanoscopic electronic devices the electron-electron interactions are particularly strong and they induce interesting many-particle effects, among them the Kondo effect which appears to be a relatively generic feature of nanodevices [4, 29, 19, 30]. As in bulk systems, the Kondo effect gives rise to vari-

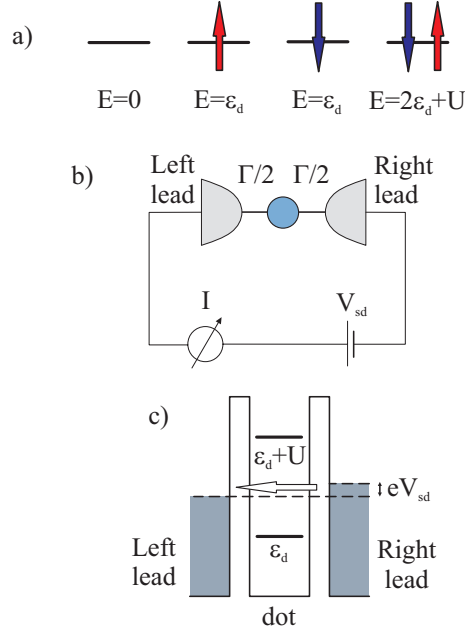


Figure 2: Representations of the single impurity Anderson model for a quantum dot.

ous anomalies in the thermodynamic and transport properties, in particular to increased conductance through nanostructures. The conductance through a quantum dot in the Kondo regime is in agreement with theoretical predictions that such dots behave rather universally as single magnetic impurities [17] and can be modelled using single impurity Anderson and Kondo models [31, 17]. Quantum dots thus serve as tunable realizations of the quantum impurity models.

3.3 Anderson impurity model

Due to electron confinement, the quantum-mechanical energy levels in a quantum dot form a series of discrete quantized levels. We focus on the electrons in the levels closest to the Fermi level in the leads, i.e. in the last occupied and first unoccupied orbital states of the dot. In the simplest case, a single electron level is relevant and a quantum dot with an odd number of confined electrons is expected to behave as a spin-1/2 magnetic impurity, similar to magnetic ions [32].

In the formalism of the second quantization, the Hamiltonian for interacting electrons in the quantum dot is

$$H_{\text{dot}} = \epsilon_d(n_{\uparrow} + n_{\downarrow}) + Un_{\uparrow}n_{\downarrow}. \quad (1)$$

ϵ_d is the energy of the electron orbital in the quantum dot (also named “on-site energy”), U is the strength of the effective electron-electron repulsion between two electrons in the same orbital, and the number operator n_{μ} is defined as $n_{\mu} = d_{\mu}^{\dagger}d_{\mu}$, where d_{μ}^{\dagger} and d_{μ} are the creation and annihilation operators; the spin index μ takes values $\mu = \pm 1/2$ or, equivalently, $\mu = \uparrow, \downarrow$. The on-site energy ϵ_d can be regulated using gate voltages which allows the charge state (occupancy) on the dots to be tuned. We may rewrite the Hamiltonian in an equivalent but more symmetric manner as

$$H_{\text{dot}} = \delta n + \frac{U}{2}(n - 1)^2, \quad (2)$$

where $n = n_\uparrow + n_\downarrow$ and $\delta = \epsilon_d + U/2$. For $\delta = 0$, the model is particle-hole symmetric and the level is occupied by a single electron on the average. The four possible configurations of the Anderson model and their energies are represented in Fig. 2a.

The conduction bands in the leads are described as

$$H_{\text{band}} = \sum_{k\mu\alpha} \epsilon_k c_{k\mu\alpha}^\dagger c_{k\mu\alpha}. \quad (3)$$

ϵ_k is the energy of an electron with wave-vector k in left ($\alpha = L$) or right ($\alpha = R$) lead described by the creation/annihilation operator pair $c_{k\mu\alpha}^\dagger$ and $c_{k\mu\alpha}$. A conduction band behaves as a sea of electrons: all states below some energy (Fermi level) are occupied, while all other high-energy states are empty. When a source-drain bias voltage V_{sd} is applied on the leads (Fig. 2b), the Fermi levels are displaced and the electrons in an energy interval of width eV_{sd} will attempt to flow from the lead with higher Fermi level through the quantum dot to the other lead, Fig. 2c. Tunneling of electrons through the junctions is described by the Hamiltonian

$$H_{\text{coupling}} = \sum_{k\mu\alpha} V_{k\alpha} (c_{k\mu\alpha}^\dagger d_\mu + d_\mu^\dagger c_{k\mu\alpha}), \quad (4)$$

where $V_{k\alpha}$ are the amplitudes for electron tunneling from lead α to the dot. The Anderson impurity model is then given by the sum $H = H_{\text{dot}} + H_{\text{band}} + H_{\text{coupling}}$.

Assuming that the coupling to the left and right electrode is equal, only symmetric combinations $c_{k\mu L}^\dagger + c_{k\mu R}^\dagger$ of conduction band electrons play a role at small bias voltage V_{sd} , while antisymmetric combinations $c_{k\mu L}^\dagger - c_{k\mu R}^\dagger$ are decoupled [23]. The use of a single channel Anderson model is then justified and the index α is unnecessary. This simplification occurs only for simple systems; in general, systems of coupled quantum dots are true multichannel quantum impurity problems.

Often the approximation of taking a constant hopping $V_k \equiv V$ is taken. Further simplification consists of considering the conduction band to have a constant density of states $\rho = 1/(2D)$, where $2D$ is the bandwidth. The hybridization strength Γ which characterizes how strongly the impurity is coupled to the conduction band is then also a constant, $\Gamma = \pi\rho V^2$.

Validity of the approximation of describing the electron in the highest occupied electron level in the quantum dot using the Anderson model has been experimentally well tested: the temperature, magnetic field and gate and bias voltage dependence of the conductance through quantum dots may be described by the simple Anderson model, however the agreement is qualitative, not quantitative [17].

In some parameter regimes, Anderson model reduces to a simpler Kondo model. Kondo model consists of a single spin in interaction with the conduction band:

$$H = \sum_{k\mu} \epsilon_k c_{k\mu}^\dagger c_{k\mu} + J\mathbf{S} \cdot \mathbf{s}(0), \quad (5)$$

where $J \approx 8V^2/U$ is the effective Kondo antiferromagnetic exchange constant, \mathbf{S} is the impurity spin-1/2 operator and $\mathbf{s}(0)$ is the spin density of the conduction band electrons at the position of the impurity. Despite their seeming simplicity, Anderson and Kondo models are both difficult many-particle problems.

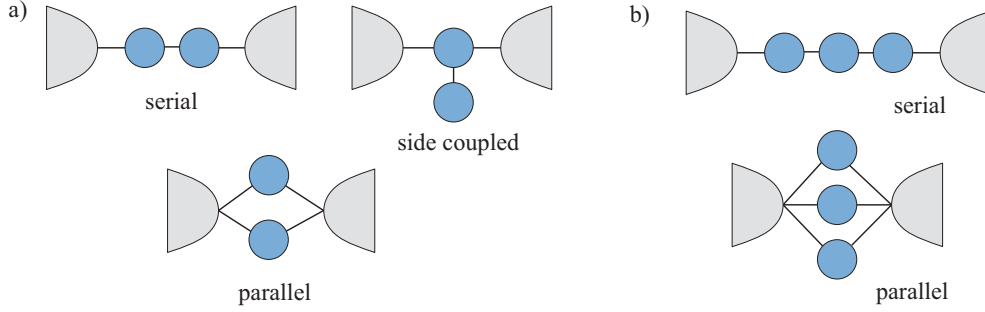


Figure 3: Representations of various multiple-impurity generalizations of the Anderson model.

3.4 Multi-impurity models

Several quantum dots (artificial atoms) can be interconnected to form an “artificial molecule” [33, 34]. Systems of multiple coupled impurities are realizations of generalized Kondo models where more exotic types of the Kondo effect may occur. The research in this field has recently intensified due to a multitude of new experimental results; the multi-impurity magnetic nanostructures under study are not only systems of multiple quantum dots [8, 35, 36, 10, 9], but also clusters of magnetic adsorbates on surfaces of noble metals (such as Ni dimers [37], Ce trimers [38] and molecular complexes [39]). Systems of two impurities are the simplest systems where one can study a number of very interesting effects, such as the effects of inter-dot electron hopping, formation of ionic or covalent inter-dot bonds, and the competition between magnetic ordering and Kondo screening, leading to quantum phase transitions [40, 41]. Recently, few-electron triple quantum dot structures have also been fabricated [11, 12] and even more complex multi-dot nanostructures can in principle also be assembled.

Systems of multiple quantum dots can be modeled by suitably generalizing the Anderson model. The properties depend in an essential way on the coupling topology, i.e. on how the various impurities are inter-connected, as represented in the examples in Fig. 3. The system can be modeled using discrete lattice models as an impurity cluster in contact with two conduction leads. Each dot (indexed by the subscript i) is described using a Hamiltonian

$$H_{\text{dot},i} = \delta_i n_i + \frac{U_i}{2} (n_i - 1)^2. \quad (6)$$

Junctions between the dots are described by “hopping Hamiltonian”

$$H_{\text{hopping}} = \sum_{\langle i,j \rangle, \mu} t_{i,j} \left(d_{i,\mu}^\dagger d_{j,\mu} + d_{j,\mu}^\dagger d_{i,\mu} \right), \quad (7)$$

and junctions between the dots and the conduction leads by suitable generalizations of Eq. (4). The impurity Hamiltonian is thus similar in form to the Hubbard model for correlated systems.

4 Theoretical tools

Most quantum impurity models are non-perturbative: the commonly used technique of expanding a problem in terms of a small perturbation around an exactly solvable non-interacting model cannot be applied in all parameter regimes due to divergences [13]. The difficulties occur in particular at low

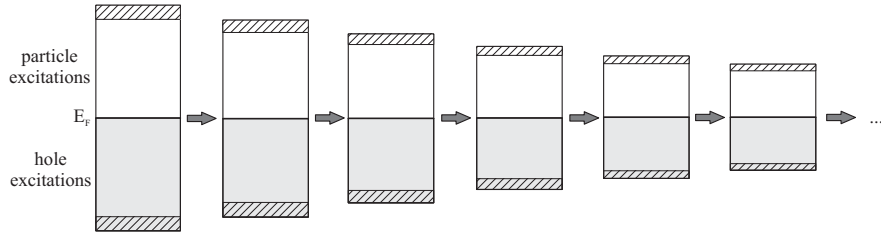


Figure 4: Cutoff renormalization: the particle and hole excitations from the hatched regions at the top and bottom of the conduction band are integrated out to obtain an effective Hamiltonian at lower energy scale.

temperatures where the systems have anomalous properties. New techniques have been developed to tackle this problem: large- N expansion [42], Bethe-Ansatz [43, 44], bosonization-refermionization [45], conformal field theory [46, 47], variational methods [48, 49] and various renormalization group techniques [50, 51, 52, 15]. Large- N techniques (such as slave-boson mean-field-theory and various improvements) allow in many cases to obtain results in closed form and often provide a qualitatively correct description; in the case of multi-impurity models, however, these methods may fail or they become impractical. Bethe-Ansatz approach provides an exact solution to the thermodynamics of the Kondo model; furthermore, very recently a method to calculate non-equilibrium dynamics was developed [53]. It seems, however, difficult to expand this approach to general multi-impurity models. Bosonization-refermionization technique has been instrumental in providing additional exact results at some special points in the parameter space, however they are less useful for exploring generic problems. Conformal field theory approach based on the non-Abelian bosonization has provided important conceptual insights into the nature of the Kondo effect: the impurity degrees of freedom are engulfed by the continuum and the only residual effect are the modified boundary conditions for continuum electron scattering at the impurity site. The actual implementation of this approach depends from case to case and has not yet been performed for complex multi-impurity problems. Variational methods were the first approach that allowed to study dynamics of quantum impurity models and has been recently generalized to multi-impurity models [54, 55, 56]. The difficulty in this approach is to correctly describe physics at very low energy scales. Since quantum impurity models become strongly renormalized at low temperatures, the development of renormalization group methods was essential in building correct understanding of the nature of the low-temperature behavior. These methods range from simple scaling of model parameters [52], to mapping to a particle gas [50, 51], and finally to Wilson’s numerical renormalization group [15, 57].

4.1 Renormalization

The renormalization is a way of describing and understanding the relation between the different ways a physical system behaves at different energy scales [58]. To study a system at low energies, the irrelevant high-energy degrees of freedom are eliminated from the problem (“integrated out”) to obtain an effective description in terms of modified, “renormalized” coupling constants g which specify the strengths of various interaction terms in the Hamiltonian, Figs. 4 and 5. The renormalization process can be described using scaling equations, which typically take the form of a system of partial differential equations

$$\partial g_j / \partial l = \beta_j(\{g_i\}), \quad (8)$$

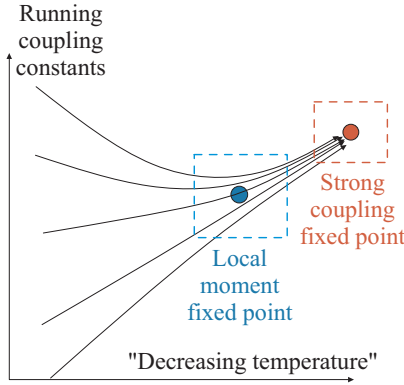


Figure 5: Schematic representation of the renormalization flow in the Anderson model. The horizontal direction represents the direction of decreasing energy scale (temperature), while the vertical direction represents the multi-dimensional space of the effective Hamiltonians (which can be considered to be parameterized by some large set of coupling constants). When the system is near a fixed point (dashed boxes), its properties can be described by a perturbative expansion around the fixed-point Hamiltonian. The diagram also illustrates the idea of universality: even for widely different original microscopic Hamiltonians, the low-temperature behavior of the systems in the same universality class is essentially the same.

where l is a “running parameter” which runs towards $-\infty$ as the energy scale is decreased and β are “beta” functions. Negative beta function corresponds to a relevant coupling constant which grows at low energies, i.e. to an interaction which becomes important at low temperatures. Positive beta function corresponds to an irrelevant coupling constant, which diminishes at low energies. If the coupling constants change only little as the renormalization procedure is performed, the system is said to be near a “fixed point”. As the temperature is reduced, the system typically crosses over several times between different fixed points which correspond to particular kinds of system’s behavior at different temperature scales, until it ultimately ends up in a stable fixed point which describes the essence of the low energy physics [58].

Generally a simple effective Hamiltonian arises from more complicated ones. A set of model Hamiltonians with the same low energy behavior constitute a universality class, see also Fig. 5. Renormalization is thus an essential ingredient in model building in many-particle theory.

4.2 Numerical renormalization group

The numerical renormalization group (NRG) was developed in 1970s by K. G. Wilson as a way of numerically exactly solving the Kondo problem [15]. It was later successfully extended to Anderson model and other quantum impurity models [59]. The NRG makes possible to compute the spectrum of excitations of the system, thermodynamic quantities such as magnetic and charge susceptibilities, entropy, and specific heat, dynamic quantities such as spectral functions, dynamical charge and spin susceptibilities, and expectation values of operators such as impurity occupancy, charge fluctuations and spin-spin correlations. The NRG is a non-perturbative method and as such does not suffer from various divergencies as other techniques do. It provides information about the behavior on all temperature scales, from the high-temperature perturbative regime to the low-temperature strong-coupling regime. It can be applied to multi-impurity and multi-channel problems; the complexity of the prob-

lem that is still manageable depends on the skillful use of the symmetries present in the problem and ultimately on the available computational resources.

The NRG consists of several steps (Fig. 6):

- Reduction of the quantum impurity problem to an effective one-dimensional problem. Since the impurity is by assumption a zero-dimensional point-like object, it always effectively couples to a continuum of states which can be parameterized by a single variable (or a finite number of such continua that we denote as “channels”).
- The one-dimensional continuum of states is discretized into bins (intervals) of geometrically decreasing widths proportional to Λ^{-m} , where the parameter Λ controls the fineness of the discretization and m is the bin index, Fig. 6a. The continuum limit is recovered for $\Lambda = 1$, while in practical calculations $\Lambda \gtrsim 2$ is used. In each interval, a spectral Fourier decomposition is performed (index l in Fig. 6a). In practical calculations, only the lowest $l = 0$ Fourier mode is retained in each interval, i.e. an interval of states is represented by the energy-averaged state. This procedure is named logarithmic discretization since the continuum degrees of freedom near the Fermi level are described with a logarithmic accuracy. A further transformation allows the problem to be formulated as an impurity attached to a one-dimensional chain of sites with exponentially decreasing hopping parameters, Fig. 6b. The sites in this chain can be interpreted as forming “onion shell”-like orbitals encircling the impurity, Fig. 6c.
- Iterative diagonalization of the chain Hamiltonian is performed, Fig. 6d. The first step consists of an exact diagonalization of the initial cluster, typically composed of the impurity sites and one chain site for each continuum channel in the problem. Additional sites are then added consecutively, one from each channel in every iteration: a new Hamiltonian is constructed and diagonalized exactly. In NRG, this procedure represents the renormalization group transformation and the iteration corresponds to the renormalization flow.
- The problem of the exponential growth of the size of the Hilbert space with the number of sites in the chain is alleviated by truncating the number of states retained at each iteration to a predefined small number of the order thousand. This turns out to be a good approximation for quantum impurity problems since there is little mixing between low-energy and high-energy excitations as the chain sites are added at each step (this property is known as the energy-scale separation).

Each iteration corresponds to the behavior of the system on a temperature scale $T_N \propto \Lambda^{-N/2}$, where N is the iteration number. The full description of the system at step N consists of the eigenstates and irreducible matrix elements for creation operators $f_{N\mu\alpha}^\dagger$ in the chain. This description is clearly much more complex compared to that in the simple renormalization approach where a small set of running coupling constants is used; the advantage is that the NRG is unbiased and, in some sense, essentially exact.

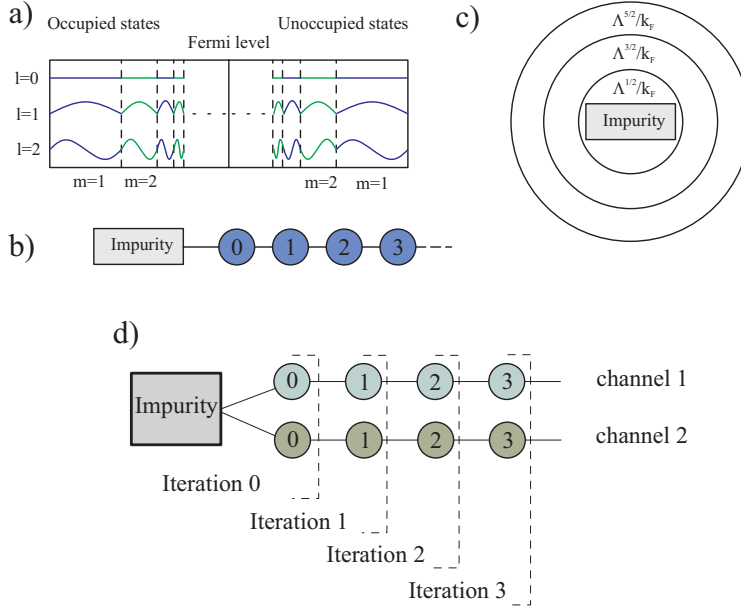


Figure 6: Numerical renormalization group. **a)** Logarithmic discretization. **b)** Chain Hamiltonian (one-channel case). **c)** Onion-shell representation of Wannier orbitals around the impurity. **d)** Chain Hamiltonians and the successive iterations in the NRG procedure: one site from each channel is added during each renormalization group transformation.

5 Quantum transport and Kondo physics

5.1 Experiments

Experiments probing fundamental properties of semiconductor quantum dots are typically performed in helium-3 dilution refrigerators at extremely low temperatures in the range of 100 mK or even less. At low temperatures, electrons occupy distinct energy levels and the Coulomb energy plays a crucial role [26]. Performing experiments at the lowest attainable temperatures is important since the energy resolution of spectroscopic techniques used is limited solely by the sample temperature [26]. Systems are characterized by performing gate-voltage and bias-voltage sweeps (gated transport spectroscopy), or by magnetic spectroscopy. This allows to obtain information about the energy levels, number of confined electrons, and electron-electron repulsion. Furthermore, finite-bias current can be approximately related to the impurity spectral function at finite frequencies.

Three elements affect the transport properties of coupled quantum dots in a characteristic manner: quantum coherence, discrete nature of the electric charge and strong electron-electron interactions.

In nanodevices made of very clean semiconductors the coherence length of electrons at low temperatures exceeds the size of the device through which the electric current flows; electrons then travel coherently through the system and behave in a wave-like manner so that quantum mechanical interference effects can occur. As the electrons scatter only off the boundaries (walls) of the device, rather than on the defects or phonons, the transport is said to be ballistic.

The conductance through nanoscopic constrictions is often found to be quantized in terms of the

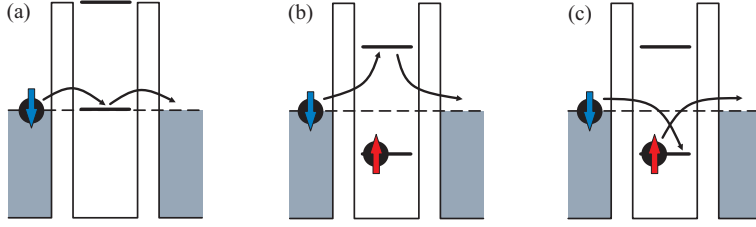


Figure 7: a) First-order tunneling, b) cotunneling, c) cotunneling with a spin-flip.

conductance quantum,

$$G_0 = 2e^2/h = e^2/\pi\hbar \approx [12.9 \text{ k}\Omega]^{-1}. \quad (9)$$

This is the conductance of a fully transmitting single-mode conduction channel taking into account both spin orientations and is experimentally measured in quantum point contacts and quantum wires. In lateral quantum dots the tunnel barriers from the 2DEG to the quantum dot are obtained by successively pinching off the propagating channels using the gate electrodes. When the last channel is pinched off, the Coulomb blockade regime develops. In this regime, only one channel from each lead is coupled to the dot.

5.2 Coulomb blockade and cotunneling

According to the analogy between a quantum dot and an atom, we expect that removing an electron from the dot (or adding it) takes energy as this is similar to the ionization of an atom. The transfer of an electron electrically charges the dot and increases the electrostatic energy by $E_C = e^2/2C$ where C is the effective capacitance between the dot and the surrounding electrodes. If the available energy is lower than the charging energy E_C (i.e. for small voltage drop across the system and for low temperature), the conductance is suppressed. This is the Coulomb blockade effect. Unless the energies of quantum dot configurations with N and $N + 1$ confined electrons happen to be aligned by suitably tuning the gate voltages (Fig. 7a), the current can flow only by cotunneling (high-order processes in hybridization strength Γ) through the virtual state with excess energy $\sim E_C$ [60, 26], Fig. 7b.

Cotunneling is an electric conduction process whereby an electron makes a virtual transition to a high-energy excited intermediate state in the quantum dot to travel from source to destination electrode in a single quantum step. It is to be opposed to a sequential tunneling process, where the electron makes a real transition to an energetically accessible state inside the device and the tunneling proceeds in two steps. Cotunneling is a characteristically quantum phenomenon related to the Heisenberg's uncertainty principle and becomes relevant at low temperatures. Occupation of the virtual state is allowed for a short time, $\sim \hbar/E$, where \hbar is the Planck constant and E the energy cost involved.

In spin-flip co-tunneling process the impurity spin is effectively flipped from spin up to spin down, or vice versa: electron with a given spin orientation tunnels in, while another electron with the opposite spin orientation tunnels out, Fig. 7c. Processes of this type are responsible for the emergence of the Kondo effect.

5.3 Conductance formulas

Particularly important transport quantity is the conductance in the limit of zero source-drain bias voltage $G = \lim_{V_{sd} \rightarrow 0} I/V_{sd}$, i.e. the linear response of the system to an imposed bias. Linear conductance is an equilibrium property of the system which can be reliably calculated for impurity models. Finite-bias problems require non-equilibrium techniques which are not yet developed to a comparable degree.

For the purpose of theoretical modeling, an electronic nanodevice may be idealized and considered as a very small scatterer embedded between two metallic contacts. According to R. Landauer, the conductance of a coherent mesoscopic device is related to the transmission probability for incident electrons [61], i.e. to the scattering properties of the impurity region. At zero temperature, the conductance is simply proportional to the transmission probability [62, 63]

$$G(T = 0) = G_0 |S_{\text{RL}}|^2, \quad (10)$$

where S_{RL} is the right-left component of the scattering matrix, i.e. the amplitude for the scattering of an electron from right to left lead.

In the vast majority of the quantum impurity problems the system behaves at low temperatures as a local Fermi liquid even if it is strongly renormalized. Fermi liquid systems are described in terms of weakly interacting quasiparticles and are fully characterized by the quasiparticle scattering phase shifts which quantify how the quasiparticles scatter in the quantum dot structure [17, 64, 65]. In the absence of the magnetic field, a single phase shift δ_{qp} per channel is required. Matrix element S_{RL} can be expressed in terms of the phase shifts and an additional angle parameter θ which depends on the symmetry of the problem, yielding the following conductance formula [66]:

$$G = G_0 \sin^2(2\theta) \sin^2(\delta_{\text{qp}}^a - \delta_{\text{qp}}^b). \quad (11)$$

For left-right symmetric problems, it is found that $\theta = \pi/4$ and that the relevant channels are formed by the symmetric (even) and antisymmetric (odd parity) linear combinations of the conduction electron states from left and right lead, so that

$$G = G_0 \sin^2(\delta_{\text{qp}}^{\text{even}} - \delta_{\text{qp}}^{\text{odd}}). \quad (12)$$

Conductance can also be computed from the impurity spectral functions using the Meir-Wingreen formula [67]:

$$G = G_0 (-\text{Im Tr} [\mathbf{\Gamma} \mathbf{G}^r]), \quad (13)$$

where $\mathbf{\Gamma}$ is a coupling matrix and \mathbf{G}^r is the matrix of retarded Green's functions of the impurity region. Green's function is essentially the Fourier transform of the probability amplitude for adding an electron to the impurity and extracting it at a later time. The imaginary part of the Green's function is the impurity spectral function. Peaks in the spectral function correspond to electronic excitations of the quantum dot and the value of the spectral function at the Fermi level is directly related to the conductance at zero temperature and can be related to the quasiparticle phase shifts in Fermi liquid systems. Meir-Wingreen formula is actually more general and it is in particular valid also for systems which are not Fermi liquids.

5.4 The Kondo effect

The Kondo effect arises due to strongly enhanced spin-flip scattering of the conduction band electrons on the impurity at low temperatures. In conventional bulk Kondo systems this leads to increased resistivity since electrons scatter isotropically in all directions which impedes the flow of the current. As a consequence, the temperature dependence of the resistivity is non-monotonic and exhibits a minimum at small temperatures, which was the first experimentally observed manifestation of the Kondo effect [14]. Curiously, in quantum dot systems the increased scattering leads to the opposite behavior: at very low temperatures the conductance increases up to the theoretical limit of one conductance quantum, G_0 , [68]. The origin of this seeming discrepancy lies in the reduced dimensionality of the problem. In quantum dot problems, scattering is effectively one-dimensional: backwards (reflection back to the lead) or forwards (transmission to the other lead). The scattering increases in forward direction, which in this case corresponds to increased electric current.

The temperature scale where the scattering increases is called the Kondo temperature, T_K . The Kondo effect is not a phase transition, but rather a cross-over, therefore the change in conductance is a very smooth function of the temperature. The Kondo temperature is a non-analytic function of model parameters, $T_K \propto \exp(-1/\rho J)$, where ρ is the density of states in the conduction band at the Fermi level and J is the effective Kondo exchange constant. It may be noted that the exponential dependence of T_K reflects the non-perturbative nature of this problem.

At temperatures much below T_K , the impurity spin is screened by the conduction band electrons and the system as a whole is non-magnetic. Properties below T_K are universal and can be described using functions of argument T/T_K ; a single parameter T_K fully characterizes the system instead of the microscopic ϵ_d, U, Γ , etc.

The Kondo exchange scattering processes generate an additional resonance in the impurity spectral function at the Fermi level. This “Kondo resonance” is of many-particle origin: the correlated behavior of a large number of electrons is required to produce it. Since properties at low temperatures are predominantly determined by the electron states near the Fermi level, the Kondo resonance significantly modifies the behavior of the system. In particular it leads to the predicted increase of the conductance through the quantum dot, Fig. 8.

The Kondo effect is clearly a magnetic effect related to electron spin. As such, it is strongly perturbed when an external magnetic field is applied. The Kondo resonance splits, the zero-bias voltage is reduced and there are two conductance peaks at finite bias. The characteristic magnetic-field dependence of the transport properties is an ultimate proof that Kondo physics is at play in a nanostructure.

6 Competing physical effects

Physical systems tend to reduce their entropy as the temperature is lowered. In the context of systems of coupled quantum impurities with spin degrees of freedom, this is most often achieved either by Kondo screening, or by magnetic ordering of some kind [69]. Both mechanism of relieving the entropy can be in competition which leads to interesting behavior [69].

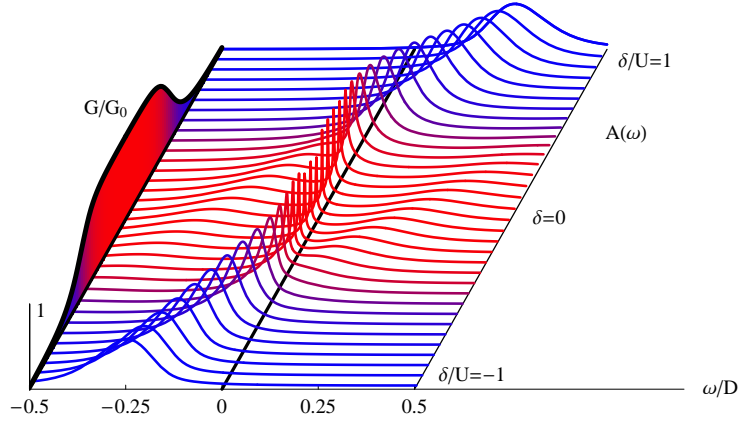


Figure 8: Spectral functions $A(\omega)$ and conductance through a quantum dot described by the single-impurity Anderson model for a range of parameters δ with $U/D = 0.5$, $\Gamma/U = 0.08$. Color of each spectral function corresponds to the value of the conductance.

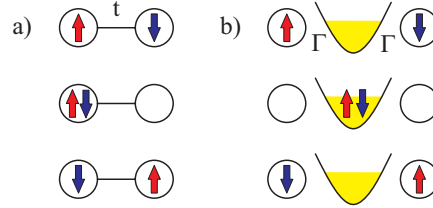


Figure 9: Processes leading to effective inter-impurity exchange interaction. a) Superexchange interaction due to electron tunneling between the dots. b) RKKY interaction mediated by the conduction band.

6.1 Inter-impurity magnetic interactions

There are several possible origins of the inter-impurity exchange interaction in quantum impurity models. One is the super-exchange mechanism which is mediated by the direct inter-impurity electron hopping (tunneling). Virtual excursions of an electron from one impurity to another modify the energy: it is reduced if the spins are anti-aligned, so that the effective exchange interaction is anti-ferromagnetic. It may be represented by an interaction term $J_{\text{eff}} \mathbf{S}_1 \cdot \mathbf{S}_2$, where \mathbf{S}_i is the impurity spin operator on dot i . For two dots decoupled from the leads, the exchange constant is given by the expression

$$J_{\text{eff}} = \frac{t}{2} \left(\sqrt{\left(\frac{U}{t}\right)^2 + 16} - \frac{U}{t} \right) \approx \frac{4t^2}{U}, \quad (14)$$

where t is the inter-impurity hopping parameter (tunneling amplitude).

Another important mechanism is the Ruderman-Kittel-Kasuya-Yosida (RKKY) effective exchange interaction. One impurity polarizes the conduction band electrons in its vicinity; these electrons in turn interact with the other impurity. The intensity and the sign of the resulting exchange interaction depends on the inter-impurity separation. It is ferromagnetic at very short distances, it oscillates with a period proportional to $1/k_F$ where k_F is the Fermi momentum, and decays as $(k_F R)^{-D}$ where D

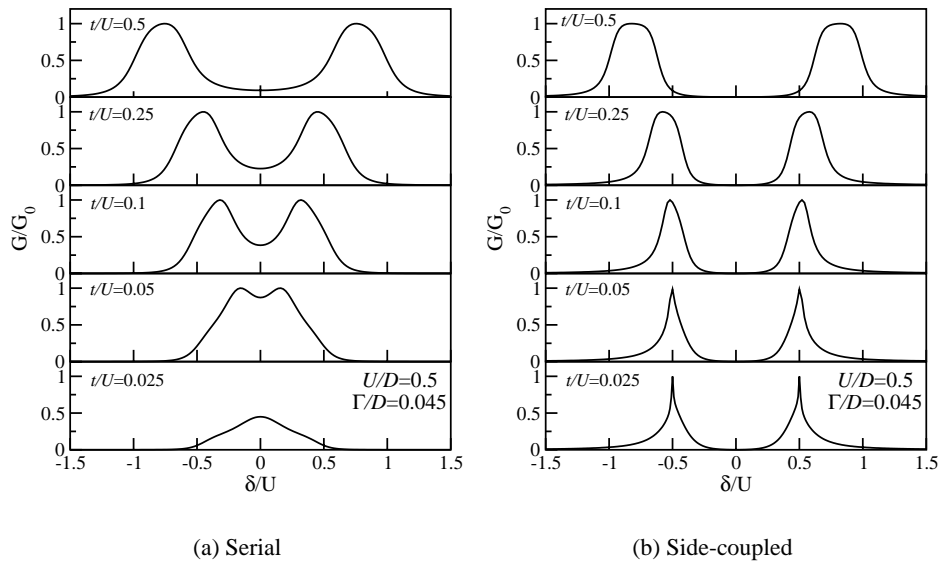


Figure 10: Zero-temperature conductance G/G_0 of the double quantum dot system in a) serial configuration and b) side-coupled configuration as a function of the gate voltage for a range of the inter-dot hopping parameters t .

is the effective dimensionality of the conduction band electron gas.

6.2 Effects of the dot-lead and inter-dot coupling topology

In multiple dot systems, the coupling of the quantum dots between each other and to the conduction leads affects the conductance in a non-trivial way since the entire system behaves in a quantum coherent way and no part of the system may be considered separately from other parts. Simple circuit theory is *not* applicable. The effects of the coupling topology can be conveniently studied in the case of double quantum dot [70]. As an illustration, we will consider the significantly different behavior of serial and side-coupled double quantum dot [70, 71].

6.2.1 Serial double quantum dot

The zero-temperature conductance of two quantum dots coupled in series between two electrodes is shown in Fig. 10a for a range of the inter-dot hopping parameters t . The conductance is calculated from the scattering phase shifts obtained in NRG calculations. For large t , the coupling between the dots is strong and the system behaves as an artificial molecule composed of two atoms. When the system is occupied by an odd number of electrons, only the unpaired electron plays an important role and the system may be mapped to an effective single-impurity Anderson model where the role of the impurity orbital is played by the bonding (symmetric) or anti-bonding (anti-symmetric) “molecular orbital”. Thus for $t/U = 0.5$, the conductance is high for $|\delta/U| = 0.5, \dots, 1.2$ when the system is occupied by 1 or 3 electrons. For $|\delta/U| < 0.5$ the conductance is low.

As t decreases, the system starts to behave as two localized magnetic moments and may be approxi-

mately described by the two-impurity Kondo model. It is found that the conductance at the particle-hole symmetric point attains the theoretical limit of G_0 at the point where the inter-impurity exchange interaction J_{eff} is comparable to the scale of the Kondo temperature for one impurity coupled to a single conduction lead, T_K , i.e. for $J_{\text{eff}} \sim T_K$ (which corresponds to $t/U \sim 0.05$, see Fig. 10a). In the true two-impurity Kondo model, this point in the parameter space corresponds to a quantum phase transition between a regime of local antiferromagnetic singlet and a regime of separate Kondo screening of each impurity moment. In the double quantum dot system, however, this quantum phase transition is replaced by a smooth cross-over due to charge transfer between the two conduction leads [72].

Finally, for very small t , the conductance tends to zero for all values of δ as the system becomes separated in two parts which no longer communicate.

6.2.2 Side-coupled double quantum dot

In the side-coupled configuration, the first quantum dot is embedded between source and drain electrodes while the second dot is coupled to the first through a tunneling junction; there is no direct coupling of the second dot to the leads. By changing the gate voltage and the inter-dot tunneling rate, this system can be tuned to one of the following low-temperature regimes: i) a non-conducting local spin-singlet state, ii) the conventional Kondo regime with odd number of electrons occupying the dots, iii) the two-stage Kondo regime with two confined electrons, or iv) a valence-fluctuating state [71]. In addition, at finite temperatures a Fano resonance appears in the conductance; its origin lies in the sudden filling of the side-coupled dot when its on-site energy crosses the Fermi level [71].

For large inter-dot tunneling coupling t , there are two wide regimes where the conductance is enhanced due to the conventional Kondo effect, for example in the ranges $|\delta/U| = 0.5, \dots, 1.5$ for $t/U = 0.5$ (Fig. 10b) when the dot is occupied by 1 or 3 electrons. These regimes are separated by a low-conductance regime where the localized spins of two electrons are antiferromagnetically coupled for $|\delta/U| \lesssim 0.5$. For large t , the side-coupled and serial configurations of quantum dots thus have qualitatively similar properties.

For small t , in the two stage Kondo regime the two local moments are screened at different Kondo temperatures [73, 74, 71, 75]. The *two-stage Kondo effect* is a generic name for successive Kondo screening of the impurity local moments at different temperatures [76, 66, 73, 77, 78, 79, 74, 71]. This term has been used in two different (but closely related) contexts: 1) two-step screening of a $S = 1$ spin in the presence of two channels [76], 2) two step screening of two local moments in the single-channel case [78, 73, 77]. In the first case, the first-stage Kondo screening is an underscreened spin-1 Kondo effect which reduces the spin to $1/2$, while the second-stage Kondo screening is a perfect-screening spin- $1/2$ Kondo effect which leads to a spin singlet ground state [80, 77]. This first case is relevant when the lowest-energy impurity configuration is a spin triplet. In the second case, at a higher Kondo temperature $T_K^{(1)}$ the Kondo effect occurs on the more strongly coupled impurity; the Fermi liquid quasiparticles associated with the Kondo effect on the first impurity participate in the Kondo screening of the second impurity on an exponentially reduced Kondo temperature scale $T_K^{(2)}$ [73, 74, 71]. This case occurs when the lowest-energy configuration is a singlet, but there is a nearby excited triplet state [78].

In the double quantum dot system, the two-stage Kondo effect occurs when the effective exchange interaction between the dots is such that $J_{\text{eff}} < T_K$, where $T_K = T_K^{(1)}$ is the Kondo temperature

of the single-impurity Anderson model that describes impurity 1 (without impurity 2) [74, 71]. The second Kondo crossover then occurs at

$$T_K^{(2)} = c_2 T_K^{(1)} \exp(-c_1 T_K^{(1)} / J_{\text{eff}}). \quad (15)$$

Constants c_1 and c_2 are of the order of 1 and they are problem-dependent. The spectral function $A_1(\omega)$ of impurity 1 increases at $\omega \sim T_K^{(1)}$, but then drops at $\omega \sim T_K^{(2)}$, i.e. there is a gap in the spectral function and the system is non-conducting at zero temperature. The conductance increases to G_0 on the temperature scale of $T_K^{(1)}$, then drops to zero on the scale of $T_K^{(2)}$. The conductance can be high at finite temperatures even in the vicinity of the particle-hole symmetric point, $\delta = 0$, if $T_K^{(2)} < T < T_K^{(1)}$.

6.3 Capacitive coupling and charge ordering

The effect of the inter-impurity electron repulsion (induced by capacitive coupling between two quantum dots) may be modeled using the following Hamiltonian term:

$$H_{\text{dots}} = \sum_{i=1}^2 H_{\text{dot},i} + U_{12}(n_1 - 1)(n_2 - 1). \quad (16)$$

The inter-impurity repulsion is not an important perturbation as long as $U_{12} < U$; finite U_{12} only modifies the Kondo temperature, while the behavior of the system remains qualitatively unchanged [81]. For $U_{12} > U$ the electrons can lower their energy by forming on-site singlets and the system enters the *charge-ordering regime* [82]. The system behaves in a peculiar way at the transition point $U_{12} = U$, when an intermediate temperature fixed point with a six-fold symmetry of states appears. In serial dots, this leads to an exotic $SU(4)$ Kondo effect [56, 82]. For parallel dots, however, the coupling of impurities to the leads breaks the orbital symmetry and conventional Kondo screening occurs [81].

7 Universal behavior versus complex particularities

Near the particle-hole symmetric point (or, equivalently, at half filling when one electron occupies each quantum dot on the average), systems consisting of even or odd number of quantum dots have radically different behavior due to the distinct properties of integer and half-integer spin states. The half-integer spin states are always degenerate and quantum dot systems with such impurity configuration tend to exhibit some form of the Kondo effect for any coupling strength; the zero-temperature conductance of systems of an odd number of dots will tend to be high. In systems with an even number of quantum dots, however, the range of half filling is generally associated with Mott-Hubbard insulating behavior [65]: the conductance for a half-filled system decreases exponentially with electron-electron repulsion U [83]. Actual behavior also crucially depends on the coupling topology. The cases of serial and parallel dots will be considered in the following.

7.1 Linear chains of quantum dots

The simplest non-trivial system with an odd number of quantum dots consists of three quantum dots coupled in series between two conduction leads. This triple quantum dot system is usually modelled as

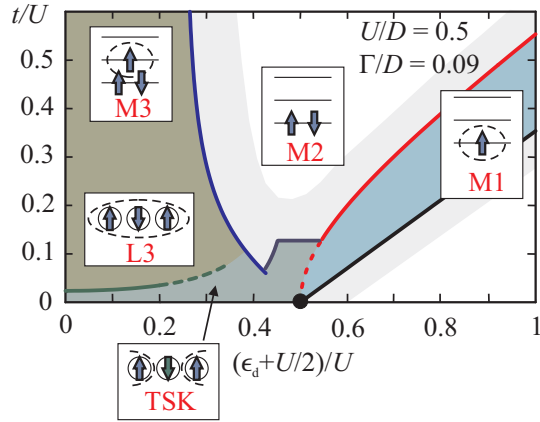


Figure 11: M1, M3: molecular-orbital Kondo regime with $\langle n \rangle \sim 1, 3$. M2: non-conductive even-occupancy state. L3: local Kondo regime with $\langle n \rangle \sim 3$. TSK: two-stage Kondo regime. Due to the particle-hole symmetry of the problem, the diagram is mirror-symmetric with respect to the $\delta = \epsilon_d + U/2 = 0$ axis; for negative $\delta < 0$ we thus find M4 non-conductive regime and M5 molecular-orbital Kondo regime.

a three-site Hubbard chain. The special feature of this system is the presence of two equivalent screening channels combined with two-stage Kondo screening and/or magnetic ordering. Triple quantum dot structures have been manufactured in recent years and the analysis of their stability diagrams demonstrates that a description in terms of a Hubbard-like model is indeed a good approximation [11, 12].

The behavior of the system depends strongly on the values of the on-site energies and on the inter-impurity hopping. Based on extensive calculations using several complementary methods, a phase diagram has been established, Fig. 11 [55]. It indicates the parameter ranges where the zero-temperature conductance is high.

For strong inter-impurity coupling t , the system may be mapped to an effective single-impurity Anderson model where the role of the impurity orbital is played by the bonding, non-bonding, or anti-bonding “molecular orbital”. In this regime, the conductance is high when the occupancy is odd, and it is nearly zero when the occupancy is even, see Fig. 12a for $t/U = 1.0, 0.5$ and 0.2 . For smaller inter-impurity coupling ($t/U \lesssim 0.1$), the molecular orbital description becomes inappropriate as the local behavior of the spins becomes important. The system then behaves as a necklace of magnetic atoms, rather than as a strongly-bound molecule.

When there are three electrons in the dots (i.e. for $\delta = 0$) and the coupling t is gradually decreased, the system crosses over from the molecular orbital M3 regime ($t \gtrsim U$) to the antiferromagnetic spin-chain L3 regime ($J_{\text{eff}} \sim t$), and finally to the two-stage Kondo (TSK) regime ($J_{\text{eff}} < T_K^{(1)}$), see Fig. 11. In the spin-chain regime, the three spins lock at $T \sim J_{\text{eff}}$ into a rigid spin-1/2 spin-chain state; at lower temperature, this collective spin is screened by the conventional spin-1/2 Kondo effect. In the two-stage Kondo regime, the spins on the first and third sites are screened at higher Kondo temperature $T_K^{(1)}$, then the spin on the central site is screened at an exponentially reduced second Kondo temperature $T_K^{(2)} \propto T_K^{(1)} \exp(-cT_K^{(1)}/J_{\text{eff}})$, where $J_{\text{eff}} \approx 4t^2/U$.

Antiferromagnetic and two-stage Kondo regimes are separated by a cross-over region with unusual

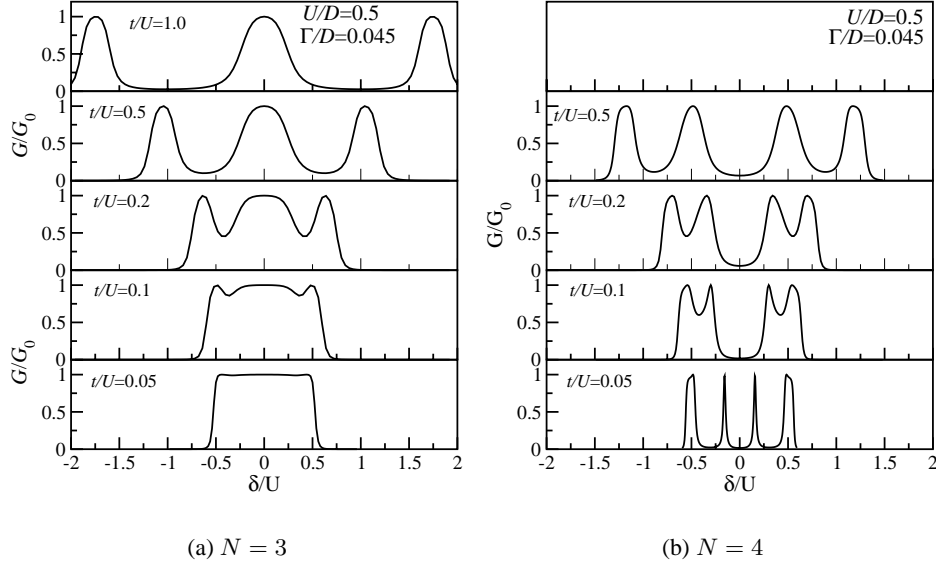


Figure 12: Conductance G/G_0 of the triple and quadruple quantum dot systems as a function of the gate voltage for a range of inter-dot hopping parameters t .

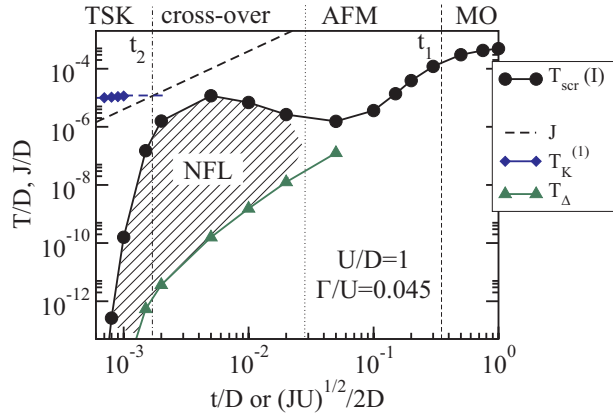


Figure 13: Cross-over scales of triple quantum dot as function of the inter-dot coupling. The magnetic screening temperature T_{scr} is defined by $T_{\text{scr}}\chi(T_{\text{scr}})/(g\mu_B)^2 = 0.07$; it is equal to the Kondo temperature when screening is due to the single-channel Kondo effect. T_{Δ} is defined through $s_{\text{imp}}(T_{\Delta})/k_B = \ln 2/4$, where $s_{\text{imp}}(T)$ is the impurity contribution to the total entropy at temperature T . Here $\ln 2/4$ is half the impurity entropy in the non-Fermi liquid fixed point.

properties at finite temperatures where the system approaches the so-called *two-channel Kondo model* non-Fermi liquid fixed point [75]. The non-Fermi liquid behavior emerges as the temperature is decreased below the Kondo temperature (T_{scr} screening temperature in Fig. 13) and disappears below the temperature T_{Δ} below which the behavior again corresponds to that of a Fermi liquid system.

Non-Fermi liquid behavior can be experimentally detected by measuring the differential conductance in a three-terminal configuration (see the insets in Fig. 14). The qualitative temperature dependence of the zero-bias conductance through the system can be approximately inferred from the frequency

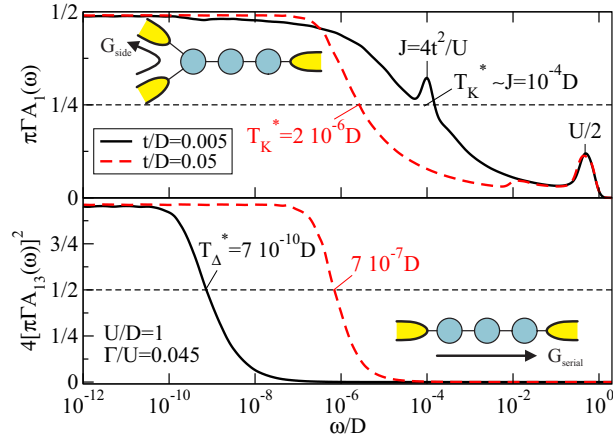


Figure 14: Dynamic properties of triple quantum dot in the antiferromagnetic (dashed lines) and in the cross-over regime (full lines). Upper panel: on-site spectral function $A_1(\omega)$ of the left dot. Lower panel: out-of-diagonal spectral function $A_{13}(\omega)$ squared. Temperature T_{Δ}^* is of order T_{Δ} , T_K^* is of order T_{scr} .

dependence of the spectral functions. The conductance through the system (from left to right conduction lead) is given by $G_{\text{serial}}/G_0 \approx 4(\pi\Gamma A_{13})^2$ (Ref. [84]) and the conductance through a side dot in the three-terminal configuration by $G_{\text{side}}/G_0 \approx \pi\Gamma A_1$ [67]. The appropriately normalized spectral densities are shown in Fig. 14 for the cases of cross-over regime with a non-Fermi liquid region and the antiferromagnetic regime with no discernible non-Fermi liquid behavior. When non-Fermi liquid fixed point is approached (for $t/D = 0.005$ and $T_{\Delta} \lesssim T \lesssim T_{scr}$), the conductance $G_{\text{side}} \sim G_0/2$, while $G_{\text{serial}} \sim 0$. The increase of the conductance G_{serial} through the system at $T \lesssim T_{\Delta}$ is concomitant with the cross-over from the non-Fermi liquid to Fermi liquid fixed point [72]. In the antiferromagnetic regime with no non-Fermi liquid region, both conductances increase below the same temperature scale, i.e. at $T \lesssim T_{scr}$.

The conductance for four quantum dots coupled in series is shown in Fig. 12b. For large t the description in terms of molecular orbitals is again appropriate and we observe four conductance peaks [65]. There is a wide region of low conductance around the particle-hole symmetric point which corresponds to the Hubbard gap, and two pairs of conductance peaks which correspond to the Hubbard sub-bands. As t is reduced, the two inner peaks become rapidly extremely sharp, while the outer peaks centered at $|\delta/U| = 1/2$ narrow down more progressively. For very small t , the system is fully insulating at zero temperature for (almost) all values of δ .

On one hand, at zero temperature short chains of even and odd number of dots in a chain are seen to have widely different properties. On the other hand, for a very large number of dots, i.e. in the limit of a macroscopic system, insulating behavior is expected at half-filling irrespective of the even or odd parity of N . These two contrasting predictions can be reconciled by considering the order of taking the $T \rightarrow 0$ and $N \rightarrow \infty$ limits [65]. Taking the $T \rightarrow 0$ limit first, the even/odd alternation is obtained. If the $N \rightarrow \infty$ limit is taken first, which is the physically correct procedure, the conductance will vanish since the Kondo temperature (at which the conductance would increase for odd N) decreases with N [65].

7.2 Parallel quantum dots

Systems of N parallel quantum dots (see Fig. 3 for $N = 2$ and $N = 3$ cases) can be described by the multi-impurity single-channel Anderson model [81]. This model is defined by $H = H_{\text{band}} + \sum_{i=1}^N H_i$, where H_{band} describes the conduction band and

$$H_i = \delta n_i + \frac{U}{2}(n_i - 1)^2 + V \sum_{k\mu} (c_{k\mu}^\dagger d_{i\mu} + d_{i\mu}^\dagger c_{k\mu}), \quad (17)$$

describe the N quantum dots.

It is assumed that all impurities hybridize with the same left-right symmetric combinations of states from both leads with a constant hybridization function $\Gamma = \pi\rho V^2$ [81]. This model may equally be applicable to other system where the RKKY interaction is ferromagnetic, for example to clusters of neighboring magnetic adatoms on metallic surfaces [38, 85, 86].

It is assumed the inter-dot tunneling coupling t and capacitive coupling (inter-dot charge repulsion) U_{12} are negligible, so that all dots are equivalent. At low temperature, the multi-impurity Anderson model maps to a multi-impurity Kondo model. At the particle-hole symmetric point, $\delta = 0$, the conduction-band-mediated RKKY exchange interaction is ferromagnetic, $\mathcal{J}_{\text{RKKY}} \sim U(\rho J_K)^2 = (64/\pi^2)(\Gamma^2/U)$, therefore the impurity spins order and the system effectively behaves as a single-impurity spin- $N/2$ Kondo model which undergoes spin- $N/2$ Kondo effect. This behavior is named the strong coupling (SC) regime. The Kondo temperature is approximately the same irrespective of the number of the impurities N . The residual spin at zero-temperature is $N/2 - 1/2$ if there is no coupling to additional screening channels. The ferromagnetically ordered regime and the ensuing spin- $N/2$ Kondo effect are fairly robust against various perturbations. Very strong perturbations lead, however, to quantum phase transitions of different kinds [81].

For very large δ/U , the impurities are unoccupied and the system is in the so-called frozen-impurity (FI) fixed-point with no residual spin. In the single-impurity ($N = 1$) case, the SC and FI fixed points are closely related: they belong to the same class of fixed points which differ in the strength of the potential scattering of the conduction band electrons on the impurity [87]. For multiple impurities ($N \geq 2$), however, the SC and FI lines of fixed points are qualitatively different (each corresponding to a different residual spin) and must be separated by at least one quantum phase transition [88].

At $\delta = 0$, the systems are fully conducting for any N and there is a wide plateau of high conductance associated with the spin- $N/2$ Kondo effect, Fig. 15 [81]. While the $N = 1$ system smoothly crosses over from the highly-conducting Kondo regime to the non-conducting FI regime, in the multi-impurity case we observe sharp conductance discontinuities: one discontinuity for N even and two discontinuities for N odd. The conductance culminates in a unitary peak slightly below $\epsilon = 0$ (i.e. below $\delta/U = 1/2$) for all $N \geq 2$. The origin of this peak is simply potential scattering. The magnetic field B has a strong effect on the Kondo plateau: the conductance is significantly reduced as soon as B is of the order of the Kondo temperature T_K . The potential scattering peak, however, is only affected by extremely high fields of the order of U .

Conductance discontinuities find their counterparts in the jumps of the total electron occupancy and spin-spin correlation functions $\langle \mathbf{S}_i \cdot \mathbf{S}_j \rangle$, $i \neq j$; a new feature, however, is the existence of two points of discontinuity for $N = 4$ even though the conductance only exhibits one. In the Kondo regime for $\delta < \delta_{c1}$, the systems are nearly half-filled and spins are ferromagnetically ordered [81]. As we cross δ_{c1} , the occupancy slightly decreases and the spin correlations turn from ferromagnetic to

antiferromagnetic. For $N \geq 3$, a second discontinuity occurs at somewhat higher δ_2 ; its characteristic property is that the occupancy changes by almost exactly $N - 2$, from $N - 1$ to 1. According to the Friedel sum rule, a change in the average total impurity occupancy by n is mirrored in a change of the scattering phase shift by $\Delta\delta_{\text{q.p.}} = n\pi/2$. This explains the conductance jump from $G = G_0 \sin^2[(N - 1)\pi/2] = 0$ to $G = G_0 \sin^2(\pi/2) = G_0$ in the case of odd $N \geq 3$ and the absence of the second conductance discontinuity for even $N \geq 4$, as 1 and $N - 1$ are both odd integers. It is remarkable that the second quantum phase transition occurs precisely at the point where the conductance is extremal.

For $N \geq 3$, the N -impurity Anderson model thus undergoes two phase transitions. The first transition separates the ferromagnetically ordered regime and associated spin- $N/2$ Kondo screening from the antiferromagnetically ordered regime and (for odd N) Kondo screening of the spin-1/2 moment [89]. The second transition reflects the instability of the phases with the occupancy in the interval $1 < \langle n_{\text{tot}} \rangle < N - 1$. Furthermore, for odd N the system abruptly switches from being fully conducting to zero conductance; this would facilitate the experimental observation of similar effects in quantum dot systems.

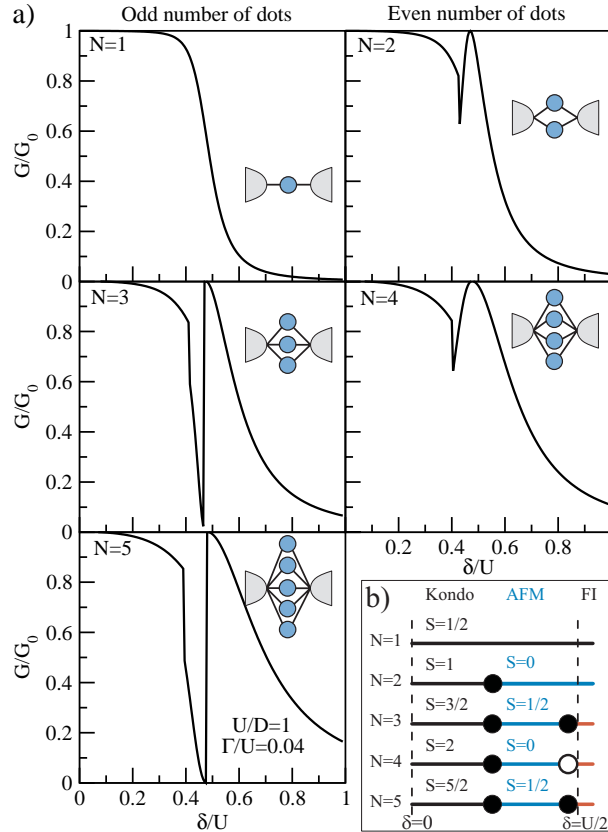


Figure 15: a) Zero-temperature conductance through systems of N parallel quantum dots as a function of the gate voltage. Only $\delta > 0$ is shown due to the symmetry of the problem. b) Zero-temperature phase diagram delimiting the different regimes as a function of the gate voltage. Filled circles (●) correspond to quantum phase transitions visible in the conductance curves, while the empty circle (○) denotes the phase transition with no associated conductance discontinuity.

8 Future directions

Further research in quantum transport theory will likely be centered at non-equilibrium, time-dependent and finite-temperature properties of interacting impurity systems. This is required to better understand transport at finite applied dc source-drain bias or for ac bias in real nanodevices. While the basic transport formalism is well developed, calculations of non-equilibrium properties of correlated system is still a formidable problem. The recently developed time-dependent NRG technique [90] appears very promising in this respect.

In recent years, the interest in quantum impurity physics has intensified once again due to an observation that extended lattice models of correlated electron systems may be exactly mapped in the limit of infinite lattice connectivity to effective impurity models subject to self-consistency conditions. This forms the foundation of a rapidly developing technique which has become known as the dynamical mean-field theory [91]. Results obtained in this way are believed to be a good approximation to the true behavior of such systems.

Experimental research is making progress toward creating artificial materials consisting of a large number of interconnected quantum dots. Studies of such systems would shed light on the behavior of extended bulk correlated materials. Furthermore, one could study how to tune material parameters to obtain desirable properties.

References

- [1] Paul L. McEuen. Artificial atoms: New boxes for electrons. *Science*, 278:1729, 1996.
- [2] Leo P. Kouwenhoven, Charles M. Marcus, Paul L. McEuen, Seigo Tarucha, Robert M. Westervelt, and Ned S. Wingreen. Electron transport in quantum dots. In L. L. Sohn, L. P. Kouwenhoven, and G. Schön, editors, *Mesoscopic electron transport*, volume 345 of *E*, pages 105–214. NATO ASI, Kluwer, Dordrecht, 1997.
- [3] Leo Kouwenhoven and Charles Marcus. Quantum dots. *Physics World*, page 35, June 1998.
- [4] D. Goldhaber-Gordon, H. Shtrikman, D. Mahalu, D. Abusch-Magder, U. Meirav, and M. A. Kastner. Kondo effect in a single-electron transistor. *Nature*, 391:156, 1998.
- [5] S. M. Cronenwett, T. H. Oosterkamp, and L. P. Kouwenhoven. A tunable kondo effect in quantum dots. *Science*, 281:540, 1998.
- [6] Leo Kouwenhoven and Leonid Glazman. Revival of the kondo effect. *Physics World*, Jan:33, 2001.
- [7] F. R. Waugh, M. J. Berry, D. J. Mar, R. M. Westervelt, K. L. Campman, and A. C. Gossard. Single-electron charging in double and triple quantum dots with tunable coupling. *Phys. Rev. Lett.*, 75:705, 1995.
- [8] H. Jeong, A. M. Chang, and M. R. Melloch. The kondo effect in an artificial quantum dot molecules. *Science*, 293:2221, 2001.
- [9] J. C. Chen, A. M. Chang, and M. R. Melloch. Transition between quantum states in a parallel-coupled double quantum dot. *Phys. Rev. Lett.*, 92:176801, 2004.

- [10] N. J. Craig, J. M. Taylor, E. A. Lester, C. M. Marcus, M. P. Hanson, and A. C. Gossard. Tunable nonlocal spin control in a coupled-quantum dot system. *Science*, 304:565, 2004.
- [11] L. Gaudreau, S. A. Studenikin, A. S. Sachrajda, P. Zawadzki, A. Kam, J. Lapointe, M. Korkusinski, and P. Hawrylak. Stability diagram of a few-electron triple dot. *Phys. Rev. Lett.*, 97:036807, 2006.
- [12] Marek Korkusinski, Irene Puerto Gimenez, Pawel Hawrylak, Louis Gaudreau, Sergei A. Studenikin, and Andrew S. Sachrajda. Topological hund's rules and the electronic properties of a triple lateral quantum dot molecule. *Phys. Rev. B*, 75:115301, 2007.
- [13] A. C. Hewson. *The Kondo Problem to Heavy-Fermions*. Cambridge University Press, Cambridge, 1993.
- [14] J. Kondo. Resistance minimum in dilute magnetic alloys. *Prog. Theor. Phys.*, 32:37, 1964.
- [15] K. G. Wilson. The renormalization group: Critical phenomena and the kondo problem. *Rev. Mod. Phys.*, 47:773, 1975.
- [16] G. R. Stewart. Heavy-fermion systems. *Rev. Mod. Phys.*, 56:755, 1984.
- [17] M. Pustilnik and L. Glazman. Kondo effect in quantum dots. *J. Phys.: Condens. Matter*, 16:R513, 2004.
- [18] J. Nygard, D. H. Cobden, and P. E. Lindelof. Kondo physics in carbon nanotubes. *Nature*, 408:342, 2000.
- [19] Wenjie Liang, Matthew P. Shores, Marc Bockrath, Jeffrey R. Long, and Kongkun Park. Kondo resonance in a single-molecule transistor. *Nature*, 417:725, 2002.
- [20] V. Madhavan, W. Chen, T. Jamneala, M. Crommie, and N. S. Wingreen. Tunneling into a single magnetic atom: Spectroscopic evidence of the kondo resonance. *Science*, 280:567, 1998.
- [21] J. Li, W.-D. Schneider, R. Berndt, and B. Delley. Kondo scattering observed at a single magnetic impurity. *Phys. Rev. Lett.*, 80:2893, 1998.
- [22] H. C. Manoharan, C. P. Lutz, and D. M. Eigler. Quantum mirages formed by coherent projection of electronic structure. *Nature*, 403:512, 2000.
- [23] L. I. Glazman and M. E. Raikh. Resonant kondo transparency of a barrier with quasilocal impurity states. *JETP Lett.*, 47:452, 1988.
- [24] T. K. Ng and P. A. Lee. On-site coulomb repulsion and resonant tunneling. *Phys. Rev. Lett.*, 61:1768, 1988.
- [25] L. P. Kouwenhoven, T. H. Oosterkamp, M. W. S. Danoesastro, M. Eto, D. G. Austing, T. Honda, and S. Tarucha. Excitation spectra of circular, few-electron quantum dots. *Science*, 278:1788, 1997.
- [26] R. C. Ashoori. Electrons in artificial atoms. *Science*, 379:413, 1996.
- [27] M. A. Kastner. The single-electron transistor. *Rev. Mod. Phys.*, 64:849, 1992.

- [28] T. J. Thornton, M. Pepper, H. Ahmed, D. Andrews, and G. J. Davies. One-dimensional conduction in the 2d electron gas of a GaAs-AlGaAs heterojunction. *Phys. Rev. Lett.*, 56:1198, 1986.
- [29] J. Park, A. N. Pasupathy, J. I. Goldsmith, C. Chang, Y. Yaish, J. R. Petta, M. Rinkoski, J. P. Sethna, H. D. Abruna, P. L. McEuen, and D. C. Ralph. Coulomb blockade and the Kondo effect in single-atom transistors. *Nature*, 417:722, 2002.
- [30] Lam H. Yu and Douglas Natelson. The Kondo effect in C_{60} single-molecule transistors. *Nanoletters*, 4:79, 2004.
- [31] J. Schmid, J. Weis, K. Eberl, and K. v. Klitzing. Absence of odd-even parity behavior for Kondo resonance in quantum dots. *Phys. Rev. Lett.*, 84:5824, 2000.
- [32] P. W. Anderson. Localized magnetic states in metals. *Phys. Rev.*, 124:41, 1961.
- [33] Gert Schedelbeck, Werner Wegscheider, Max Bichler, and Gerhard Abstreiter. Coupled quantum dots fabricated by cleaved edge overgrowth: From artificial atoms to molecules. *Science*, 278:1792, 1997.
- [34] T. H. Oosterkamp, T. Fujisawa, W. G. van der Wiel, K. Ishibashi, R. V. Hijman, S. Tarucha, and L. P. Kouwenhoven. Microwave spectroscopy of a quantum-dot molecule. *Nature*, 395:873, 1998.
- [35] A. W. Holleitner, R. H. Blick, A. K. Hüttel, K. Eberl, and J. P. Kotthaus. Probing and controlling the bonds of an artificial molecule. *Science*, 297:70, 2002.
- [36] W. G. van der Wiel, S. De Franceschi, J. M. Elzerman, T. Fujisawa, S. Tarucha, and L. P. Kouwenhoven. Electron transport through double quantum dots. *Rev. Mod. Phys.*, 75:1, 2003.
- [37] V. Madhavan, T. Jamneala, K. Nagaoka, W. Chen, Je-Luen Li, S. G. Louie, and M. F. Crommie. Observation of spectral evolution during the formation of $n_{\uparrow}n_{\downarrow}$ Kondo molecule. *Phys. Rev. B*, 66:212411, 2002.
- [38] T. Jamneala, V. Madhavan, and M. F. Crommie. Kondo response of a single antiferromagnetic chromium trimer. *Phys. Rev. Lett.*, 87:256804, 2001.
- [39] P. Wahl, L. Diekhoner, G. Wittich, L. Vitali, M. A. Schneider, and K. Kern. Kondo effect of molecular complexes at surfaces: ligand control of the local spin coupling. *Phys. Rev. Lett.*, 95:166601, 2005.
- [40] B. A. Jones, C. M. Varma, and J. W. Wilkins. Low-temperature properties of the two-impurity Kondo Hamiltonian. *Phys. Rev. Lett.*, 61:125, 1988.
- [41] I. Affleck, A. W. W. Ludwig, and B. A. Jones. Conformal-field-theory approach to the two-impurity Kondo problem: Comparison with numerical renormalization-group results. *Phys. Rev. B*, 52:9528, 1995.
- [42] N. E. Bickers. Review of techniques in the large- n expansion for dilute magnetic alloys. *Rev. Mod. Phys.*, 59:845, 1987.
- [43] N. Andrei, K. Furuya, and J. H. Lowenstein. Solution of the Kondo problem. *Rev. Mod. Phys.*, 55:331, 1983.

- [44] A. M. Tsvelick and P. B. Wiegmann. Exact results in the theory of magnetic alloys. *Adv. Phys.*, 32:453, 1983.
- [45] Alexander O. Gogolin, Alexander A. Nersesyan, and Alexei M. Tsvelik. *Bosonization and strongly correlated systems*. Cambridge University Press, 1999.
- [46] I. Affleck. A current algebra approach to the kondo effect. *Nucl. Phys. B*, 336:517, 1990.
- [47] I. Affleck and Andreas W. W. Ludwig. The kondo effect, conformal field theory and fusion rules. *Nucl. Phys. B*, 352:849, 1991.
- [48] C. M. Varma and Y. Yafet. Magnetic susceptibility of mixed-valence rare-earth compounds. *Phys. Rev. B*, 13:2950, 1976.
- [49] O. Gunnarsson and K. Schönhammer. Electron spectroscopies for ce compounds in the impurity model. *Phys. Rev. B*, 28:4315, 1983.
- [50] P. W. Anderson and G. Yuval. Exact results in the kondo problem: Equivalence to a classical one-dimensional coulomb gas. *Phys. Rev. Lett.*, page 89, 1969.
- [51] P. W. Anderson, G. Yuval, and D. R. Hamann. Exact results in the kondo problem ii: Scaling theory, qualitatively correct solution and some new results on one-dimensional classical statistical models. *Phys. Rev. B*, 1:4464, 1970.
- [52] P. W. Anderson. A poor man's derivation of scaling laws for the kondo problem. *J. Phys. C: Solid St. Phys.*, 3:2436, 1970.
- [53] Pankaj Mehta and Natan Andrei. Nonequilibrium transport in quantum impurity models: The bethe ansatz for open systems. *Phys. Rev. Lett.*, 96:216802, 2006.
- [54] T. Rejec and A. Ramšak. Formulas for zero-temperature conductance through a region with interaction. *Phys. Rev. B*, 68:035342, 2003.
- [55] R. Žitko, J. Bonča, A. Ramšak, and T. Rejec. Kondo effect in triple quantum dots. *Phys. Rev. B*, 73:153307, 2006.
- [56] J. Mravlje, A. Ramšak, and T. Rejec. Kondo effect in double quantum dots with interdot repulsion. *Phys. Rev. B*, 73:241305(R), 2006.
- [57] Ralf Bulla, Theo Costi, and Thomas Pruschke. cond-mat/0701106, 2007.
- [58] P. Coleman. Local moment physics in heavy electron systems. cond-mat/0206003, 2002.
- [59] H. R. Krishna-murthy, J. W. Wilkins, and K. G. Wilson. Renormalization-group approach to the anderson model of dilute magnetic alloys. i. static properties for the symmetric case. *Phys. Rev. B*, 21:1003, 1980.
- [60] D. V. Averin and Yu. V. Nazarov. Virtual electron diffusion during quantum tunneling of the electric charge. *Phys. Rev. Lett.*, 65:2446, 1990.
- [61] Yoseph Imry and Rolf Landauer. Conductance viewed as transmission. *Rev. Mod. Phys.*, 71:S306, 1999.

- [62] Yoseph Imry. *Introduction to mesoscopic physics*. Oxford University Press, second edition, 2002.
- [63] Supriyo Datta. *Electronic Transport in Mesoscopic Systems*. Cambridge University Press, 1997.
- [64] Akira Oguri, Yunori Nisikawa, and A. C. Hewson. Determination of the phase shifts for interacting electrons connected to reservoirs. *J. Phys. Soc. Japan*, 74:2554, 2005.
- [65] Yunori Nisikawa and Akira Oguri. Numerical renormalization group approach to a quartet quantum-dot array connected to reservoirs: Gate-voltage dependence of the conductance. *Phys. Rev. B*, 73:125108, 2006.
- [66] M. Pustilnik and L. I. Glazman. Kondo effect in real quantum dots. *Phys. Rev. Lett.*, 87:216601, 2001.
- [67] Y. Meir and N. S. Wingreen. Landauer formula for the current through an interacting electron region. *Phys. Rev. Lett.*, 68:2512, 1992.
- [68] W. G. van der Wiel, S. De Franceschi, T. Fujisawa, J. M. Elzerman, S. Tarucha, and L. P. Kouwenhoven. The kondo effect in the unitary limit. *Science*, 289:2105, 2000.
- [69] M. Fabrizio. Clusters of anderson impurities and beyond: How kondo effect dies and what can we learn about the mott transition. Lecture notes, XI Training Course in the Physics of Strongly Correlated Systems, 2006.
- [70] A. Ramšak, J. Mravlje, R. Žitko, and J. Bonča. Spin qubits in double quantum dots: Entanglement versus the kondo effect. *Phys. Rev. B*, 74:241305(R), 2006.
- [71] R. Žitko and J. Bonča. Enhanced conductance through side-coupled double quantum dots. *Phys. Rev. B*, 73:035332, 2006.
- [72] Gergely Zaránd, Chung-Hou Chung, Pascal Simon, and Matthias Vojta. Quantum criticality in a double quantum-dot system. *Phys. Rev. Lett.*, 97:166802, 2006.
- [73] M. Vojta, R. Bulla, and W. Hofstetter. Quantum phase transitions in models of coupled magnetic impurities. *Phys. Rev. B*, 65:140405(R), 2002.
- [74] P. S. Cornaglia and D. R. Grempel. Strongly correlated regimes in a double quantum dot device. *Phys. Rev. B*, 71:075305, 2005.
- [75] Rok Žitko and Janez Bonča. Fermi-liquid versus non-fermi-liquid behavior in triple quantum dots. *Phys. Rev. Lett.*, 98:047203, 2007.
- [76] C. Jayaprakash, H. R. Krishna-murthy, and J. W. Wilkins. Two-impurity kondo problem. *Phys. Rev. Lett.*, 47:737, 1981.
- [77] W. G. van der Wiel, S. De Franceschi, J. M. Elzerman, S. Tarucha, L. P. Kouwenhoven, J. Motohisa, F. Nakajima, and T. Fukui. Two-stage kondo effect in a quantum dot at a high magnetic field. *Phys. Rev. Lett.*, 88:126803, 2002.
- [78] W. Hofstetter and H. Schoeller. Quantum phase transition in a multilevel dot. *Phys. Rev. Lett.*, 88:016803, 2002.

- [79] W. Hofstetter and G. Zarand. Singlet-triplet transition in lateral quantum dots: A renormalization group study. *Phys. Rev. B*, 69:235301, 2004.
- [80] Walter Hofstetter. Generalized numerical renormalization group for dynamical quantities. *Phys. Rev. Lett.*, 85:1508, 2000.
- [81] Rok Žitko and Janez Bonča. Multi-impurity anderson model for quantum dots coupled in parallel. *Phys. Rev. B*, 74:045312, 2006.
- [82] M. R. Galpin, D. E. Logan, and H. R. Krishnamurthy. Quantum phase transition in capacitively coupled double quantum dot. *Phys. Rev. Lett.*, 94:186406, 2005.
- [83] A. Oguri and A. C. Hewson. Nrg approach to the transport through a finite hubbard chain connected to reservoirs. *J. Phys. Soc. Japan*, 74:988, 2005.
- [84] C. Caroli, R. Combescot, P. Nozieres, and D. Saint-James. Calculation of the tunneling current. *J. Phys. C*, 4:916, 1971.
- [85] A. A. Aligia. Effective kondo model for a trimer on a metallic surface. *Phys. Rev. Lett.*, 96:096804, 2006.
- [86] P. Wahl, P. Simon, L. Diekhöner, V. S. Stepanyuk, P. Bruno, M. A. Schneider, and K. Kern. Exchange interaction between single magnetic adatoms. *Phys. Rev. Lett.*, 98:056601, 2007.
- [87] H. R. Krishna-murthy, J. W. Wilkins, and K. G. Wilson. Renormalization-group approach to the anderson model of dilute magnetic alloys. ii. static properties for the asymmetric case. *Phys. Rev. B*, 21:1044, 1980.
- [88] Matthias Vojta. Impurity quantum phase transitions. *Phil. Mag.*, 86:1807, 2006.
- [89] Rok Žitko and Janez Bonča. Quantum phase transitions in systems of parallel quantum dots, 2007.
- [90] F. B. Anders and A. Schiller. Real-time dynamics in quantum impurity systems: A time-dependent numerical renormalization group approach. *Phys. Rev. B*, 74:245113, 2006.
- [91] Gabriel Kotliar. Quantum impurity models as reference systems for strongly correlated materials: the road from the kondo impurity model to first principles electronic structure calculations with dynamical mean-field theory. *J. Phys. Soc. Japan*, 74:147, 2005.